Journal of Physics: Conference Series

PAPER • OPEN ACCESS

Generalization of numerical simulation results on the electrical coalescence threshold for two conducting droplets based on non-dimensional parameters

To cite this article: V A Chirkov and P A Kostin 2024 *J. Phys.: Conf. Ser.* **2701** 012075

View the article online for updates and enhancements.

You may also like

- Frequency-dependent transient response of an oscillating electrically actuated droplet
S Dash, N Kumari and S V Garimella
- Ostwald ripening in macro- and nanoemulsions
Marina Yu. Koroleva and Evgeny V. Yurtov
- Comparing Modelling and Experiments for Prediction of Atmospheric Corrosion Under Controlled Dynamic Thin Film and Droplet Electrolytes
Herman Albert Terryn, Nils Van Den Steen, Keer Zhang et al.

This content was downloaded from IP address 195.19.233.35 on 29/02/2024 at 06:00

Generalization of numerical simulation results on the electrical coalescence threshold for two conducting droplets based on non-dimensional parameters

V A Chirkov and P A Kostin

St. Petersburg State University, St. Petersburg, Russia
v.chirkov@spbu.ru

Abstract. Electrocoalescence, the physical process underlying the demulsification of a dielectric dispersion medium containing small conductive droplets (e.g., water), involves droplet merging at low electric fields and splashing at higher voltages. Understanding the physics of electrocoalescence is crucial for optimizing industrial electrocoalescers. However, mathematical modeling of these complex, multiphysics phenomena is challenging, and many published results are questionable. In this study, we utilized a previously developed reliable model for computing the threshold between electrical coalescence and non-coalescence. We investigate the applicability of dimensionless parameters, such as the Ohnesorge number and Weber electric number, to describe the coalescence threshold for uncharged droplets of equal size. Using COMSOL Multiphysics software, we analyze the dependency of the threshold electric field strength on water droplet radius and establish an equivalent dimensionless relationship. Our findings reveal that a universal Weber number quite accurately describes the threshold over a wide range of droplet radii, regardless of changes in liquid viscosity and inter-electrode gap. Direct mathematical simulations using up-to-date numerical models enable us to determine non-dimensional parameter values corresponding to the threshold electric field strength, providing generalizable results.

1. Introduction

Electrocoalescence, also known as electrically-induced coalescence, is a phenomenon that occurs when electric fields are applied to immiscible liquids. This process involves the merging of dispersed droplets under the effect of electrical forces, leading to the formation of larger entities. Electrocoalescence has gained considerable attention in recent years due to its relevance in a wide range of industrial applications, including oil-water separation and electrochemical processes. Understanding the complex dynamics and underlying mechanisms of electrocoalescence is crucial for optimizing industrial processes and developing efficient separation techniques. However, studying this phenomenon experimentally can be challenging due to the difficulty of controlling various parameters and observing the underlying processes at a microscopic level. In this regard, numerical simulations have emerged as valuable tools for unraveling the intricacies of electrocoalescence, offering a cost-effective and controllable means to explore the behavior of dispersed phases under different conditions. A detailed description of the current state of affairs in the study of electrocoalescence is provided in [1].


Content from this work may be used under the terms of the Creative Commons Attribution 3.0 licence. Any further distribution of this work must maintain attribution to the author(s) and the title of the work, journal citation and DOI.
Published under licence by IOP Publishing Ltd

Modeling electrocoalescence processes is a challenging task, and the applicability of some utilized models raises questions regarding the results obtained. Questions about applicability arise, for example, in cases where the conducting phase does not have the same electrical potential [2,3], and when surface charge is located not at the interface [4]. These issues are discussed in more detail in [5]. In this work, we utilize a previously tested and validated physical model [6].

To enhance the applicability and generalization of results obtained through numerical simulations or experiments, the dimensionless parameters are used. The dimensionless parameters allow researchers to systematically investigate the influence of various factors, such as droplet size, electrical field strength, and fluid properties, while eliminating the dependence on specific units and scales. Among the dimensionless parameters commonly employed in the study of electrocoalescence, the Ohnesorge number, electrical Weber number and Bond number have proven to be particularly valuable tools. The Ohnesorge number (*Oh*) characterizes the competition between viscous forces and surface tension. The electrical Weber number (We), also known as electric Bond number or electric capillary number, which compares the electrical forces acting on the droplet to the surface tension, elucidates the relative importance of electrical forces in the coalescence process. The electric Bond number should be distinguished from the Bond number (*Bo*), which characterizes the relative importance of gravitational forces to surface tension forces.

Thus, in [7], researchers constructed a diagram in *Oh* and *Bo* coordinates to differentiate between complete and partial coalescence cases for the droplet-film system in the absence of an electric field. In [8], the authors rely on the values of *Oh* and *We* to study the droplet-film system in the presence of an electric field. In the study [9], Oh^2 is utilized for the same purpose. The article [10] investigates the influence of *We* on the coalescence process in the droplet-film system through numerical simulations. In [11,12], different coalescence regimes are attempted to be distinguished for the droplet-droplet system without an electric field using the *Oh* number. The article [13] defines the critical value of the electric capillary number for various frequencies of the external field. In [4,14] researchers aim to characterize the size of the secondary droplet formed during partial coalescence using the ratio *We*/*Oh* and the product *We***Oh*, respectively.

In the study [15], a linear dependence of the critical field strength on the droplet radius raised to the power of −0.5 has been experimentally observed for the droplet-film system.

In this article, our main objective is to investigate the relationship between droplet radius and the electric field strength threshold between coalescence and non-coalescence. By systematically varying the radius of the droplets and manipulating the fluid properties, we aim to elucidate the impact of these factors on the critical electrical Weber number.

2. Numerical model

This section presents the mathematical model employed to calculate the coalescence process. Initially, the model is formulated without the use of dimensionless parameters. Subsequently, dimensionless parameters are introduced, and the parameter range for problem formulation is described.

2.1. Original model

The model is formulated considering the following simplifications: isothermality of the medium, much lower conductivity of the medium compared to water conductivity. Additionally, uncharged droplets of the same size are considered, and the line connecting the centers of the droplets is aligned with the electric field. Gravity is not taken into account. The equations being solved are as follows:

$$\rho_1\left(\frac{\partial \boldsymbol{v}}{\partial t} + (\boldsymbol{v}, \boldsymbol{\nabla})\boldsymbol{v}\right) = -\boldsymbol{\nabla} p + \eta_1 \Delta \boldsymbol{v} \quad outside \quad \Omega \tag{1.1}$$

$$\rho_2\left(\frac{\partial \boldsymbol{v}}{\partial t} + (\boldsymbol{v}, \boldsymbol{\nabla})\boldsymbol{v}\right) = -\boldsymbol{\nabla} p + \eta_2 \Delta \boldsymbol{v} \quad inside \quad \Omega \tag{1.2}$$

$$(\boldsymbol{\nabla}, \boldsymbol{v}) = 0 \tag{1.3}$$

$$p_2 - p_1 = f_{st} + f_{el},\ f_{st} = -2\sigma\kappa,\ f_{el} = \frac{1}{2}\varepsilon_1 E^2 \quad on \quad \partial\Omega \tag{1.4}$$

The electric field strength $\boldsymbol{E}$ is determined from an additional equation:

$$\Delta\varphi = 0, \boldsymbol{E} = -\boldsymbol{\nabla}\varphi \tag{1.5}$$

The boundary conditions are depicted in Figure 1.
The following notations are used:

- The computational variables: $\boldsymbol{v}$—velocity, p—pressure, φ—electric potential.
- Derived quantities from the computational variables: f_{st}—surface tension force, f_{el}—electrostatic pressure (the Coulomb force), κ—surface curvature, $\boldsymbol{E}$—electric field strength.
- The material properties: ρ—mass density, η—dynamic viscosity, σ—interfacial tension, ε—absolute permittivity. Index 1 refers to the medium, and index 2 refers to the water droplet.
- Ω is an area occupied by the water droplet and $\partial\Omega$—a boundary of this area.

The displacement of a water droplet in medium is accomplished using the Arbitrary Lagrangian-Eulerian (ALE) method, also known as the moving mesh method. The problem is solved in two stages: droplet approach and the evolution of droplets with a connecting bridge. The bridge is manually added by modifying the geometry, with a height and diameter $0.01r_0$ where r_0 is the droplet radius. The initial distance between edges of droplets is $2r_0$. The problem solution is implemented in Comsol Multiphysics. The model has been verified and validated in the study [6].

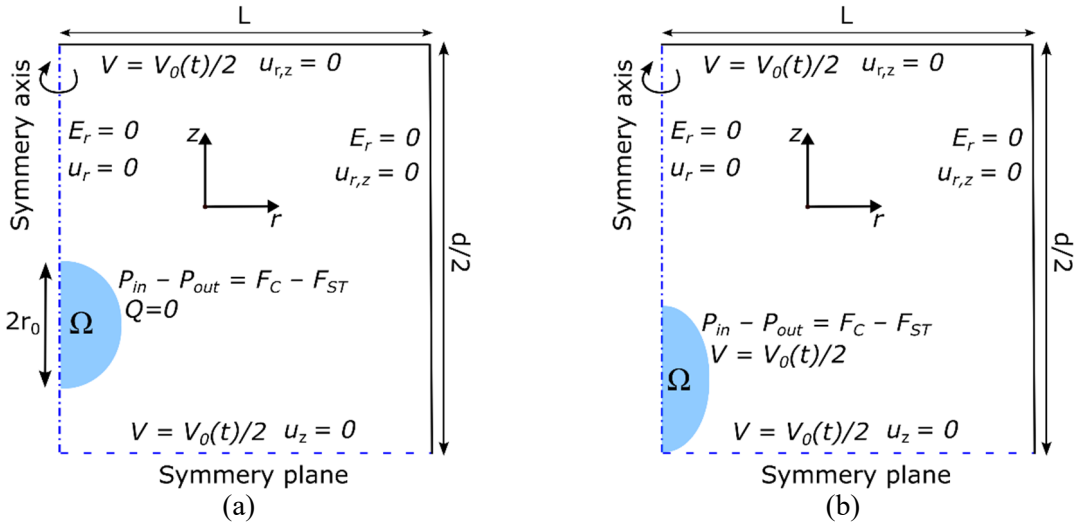

Figure 1. A schematic representation of the model geometry and boundary conditions. (a)—Stage 1: approach of droplets, (b)—Stage 2: coalescence attempt.

2.2. Dimensionless numbers

The non-dimensionalization of the set of equations (1) is performed as follows. Dimensional scales are introduced for each variable. Then, in the equations, the variables are replaced by the product of the corresponding non-dimensional variable and scale. For this system of equations, the following scales are used: for the spatial coordinates r_0—the initial droplet radius, for time—$t_0 = \rho_1 r_0^2/\eta_1$, pressure—$p_0 = \sigma/r_0$, velocity—$v_0 = \sigma/\eta_1$, electric potential—$\varphi_0 = E_0 r_0$. These scales lead the original system of equations to the following non-dimensional system. For convenience, the non-dimensional variables are denoted by the same symbols as the dimensional variables in the previous system (1).

$$\frac{\partial \boldsymbol{v}}{\partial t} + \frac{1}{Oh^2}(\boldsymbol{v}, \boldsymbol{\nabla})\boldsymbol{v} = -\boldsymbol{\nabla} p + \Delta \boldsymbol{v} \;\; outside\; \Omega \tag{2.1}$$

$$k_\rho \frac{\partial \boldsymbol{v}}{\partial t} + k_\rho \frac{1}{Oh^2}(\boldsymbol{v}, \boldsymbol{\nabla})\boldsymbol{v} = -\boldsymbol{\nabla} p + k_\eta \Delta \boldsymbol{v} \;\; inside \;\; \Omega \tag{2.2}$$

$$(\boldsymbol{\nabla}, \boldsymbol{v}) = 0 \tag{2.3}$$

$$p_2 - p_1 = -2\kappa + \frac{1}{4} We \cdot E^2 \;\; on \;\; \partial\Omega \tag{2.4}$$

$$\Delta \varphi = 0, \boldsymbol{E} = -\boldsymbol{\nabla}\varphi \tag{2.5}$$

From the boundary conditions on the potential, the following expressions arise: $\varphi = k_d$ at the upper boundary and $\varphi = k_d/2$ on the symmetry plane (antisymmetry for the electric potential).

Here, the following parameters are introduced:

$$Oh = \frac{\eta_1}{\sqrt{\sigma \rho_1 r_0}}, \; We = \frac{2\varepsilon_1 r_0 E_0^2}{\sigma} \tag{3}$$

$$k_\rho = \frac{\rho_2}{\rho_1}, \; k_\eta = \frac{\eta_2}{\eta_1}, \; k_L = \frac{d}{r_0} \tag{4}$$

The parameters may vary depending on the constants and are commonly chosen in a form frequently encountered in the literature. It should be noted that in general, for droplets of different radii and when the line connecting their centers does not align with the field direction, additional parameters will arise.

2.3. Model Parameters

The original system of equations is used to determine the threshold between coalescence and non-coalescence for a given initial droplet radius r_0. In other words, the objective is to find a value of the electric field intensity E_0, such that coalescence occurs below this threshold and non-coalescence occurs above it.

The range for the Ohnesorge number is estimated in the following manner. For petroleum and oils, the typical viscosity ranges from 10 to 100 mPa·s, interfacial tension ranges from 5 to 50 mN/m, water droplet radius ranges from 50 μm to 1 mm, and the density is approximately fixed at 1000 kg/m^3. This yields an Ohnesorge number ranging approximately from 0.01 to 10. For the purposes of this work, we limit the range of Ohnesorge number to 0.05 to 5.

For a given Ohnesorge number, we compute the corresponding droplet radius r_0, using the fluid properties. Subsequently, a series of problems are solved for this radius, with the average field strength, E_0, varied. The aim is to find the value of E_0 that corresponds to the threshold. This is achieved by determining the values of E_{coal} and $E_{non-coal}$ such that their relative difference does not exceed 1%.

The main calculations were conducted for two low-conducting liquids: Polydimethylsiloxane (PDMS50) and olive oil; the second phase is water in both cases. The properties of these liquids are presented in table 1.

Table 1. Material properties

Liquid	PDMS50	Olive oil	Water
Density, kg/m^3	958	909.5	1000
Dynamic viscosity, mPa s	49.1	68.45	1
Interfacial tension (against water), mN/m	39	15.8	
Relative permittivity, 1	2.59	2.85	

Let's consider the dimensions of the cuvette separately. In reality, different options may be required. For example, in large industrial electrocoalescers, the dimensions of the inter-electrode gap are much larger than the droplet radius. In laboratory experiments, the droplet sizes may be comparable to the size of the inter-electrode gap. In the former case, the parameter $k_d = d/r_0$ becomes much larger than unity, and

its influence can be neglected. This option was used in the main part of the modeling, specifically with a fixed value of $k_d = 50$. To examine the effect of cuvette size on the results, a scenario with a fixed $d = 30$ mm was studied. Therefore, in the latter case, the parameter k_d will vary for different droplet radii.

3. Results and discussion

This section thoroughly examines the dependence of the critical field intensity on the droplet radius. First, the rationale for introducing dimensionless parameters is discussed using the example of PDMS50 liquid. Then, the observed dependency is compared to that of another liquid, olive oil. Subsequent sections investigate the influence of viscosity and cuvette size on the observed dependency.

3.1. Dependence of threshold on droplet radius

Let's consider the coalescence problem using the example of PDMS50 liquid. The illustration in Figure 2 depicts the solution. At the initial moment, two droplets are separated by a certain distance (Figure 2a). After applying the electric field, they are attracted to each other through dipole-dipole interactions and undergo deformation (Figure 2b). When the distance between the droplets decreases to a selected critical value of $0.01r_0$, a thin bridge is formed between them (Figure 2b 2)). Subsequently, the droplets can either merge (Figure 2c) or separate into two or more droplets, leading to non-coalescence. Typically, two types of non-coalescence are observed: the division into two larger droplets with a small central droplet (Figure 2e), occurring for small radii, and the dispersion of small droplets from the ends of a merged larger droplet (Figure 2d), occurring for larger radii.

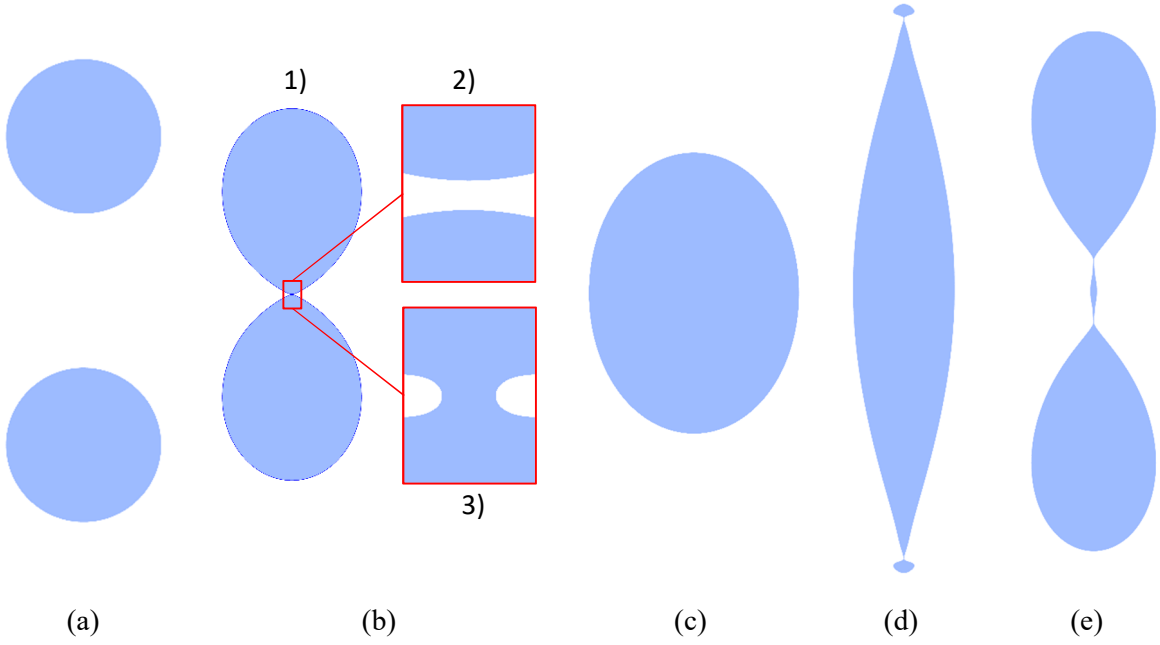

Figure 2. Illustrations of typical droplet shapes (direct simulation results). (a)—initial state; (b)—coalescence attempt: 1) general view, 2) before bridge formation 3) after bridge formation; (c)—coalescence; (d)—non-coalescence with dispersion; (e)—non-coalescence with central droplet formation.

A search for the threshold between coalescence and non-coalescence was conducted for a range of radii corresponding to *Oh* values ranging from 0.05 to 5. The results are presented in Figure 3a using a logarithmic scale for both axes. The obtained data points are well approximated by a linear relationship $\lg E = a + b \lg R$, where the approximation coefficients are $a = 0.6, b = -0.5$, indicating $E \sim r_0^{-0.5}$. It should be noted, that the same relationship was previously introduced for the system droplet-film in [15].

The discovered relationship serves as a basis for introducing dimensionless parameters. For $r_0^{-0.5}$, the dimensionless analogue is the Oh number. To non-dimensionalize *E*, we introduce a new parameter *DE*, which represents the dimensionless electric field strength:

$$DE = \sqrt{We}Oh = \sqrt{\frac{2\varepsilon_1 r_0 E_0^2}{\sigma}\frac{\eta_1}{\sqrt{\sigma\rho_1 r_0}}} = E_0\sqrt{\frac{2\varepsilon_1\eta_1^2}{\rho_1\sigma^2}} \quad (5)$$

DE parameter is proportional to the electric field strength, where the proportionality coefficient is determined by the material properties.

The dependence of *DE* on *Oh* is shown in Figure 3b. This dependence is accurately approximated by the function $DE = a \cdot Oh$, where $a = 0.42$. Therefore, it can be inferred that $\sqrt{We}Oh = a \cdot Oh$, implying that the coalescence threshold is reached at a fixed value of *We*, equal to $a^2 = 0.178$.

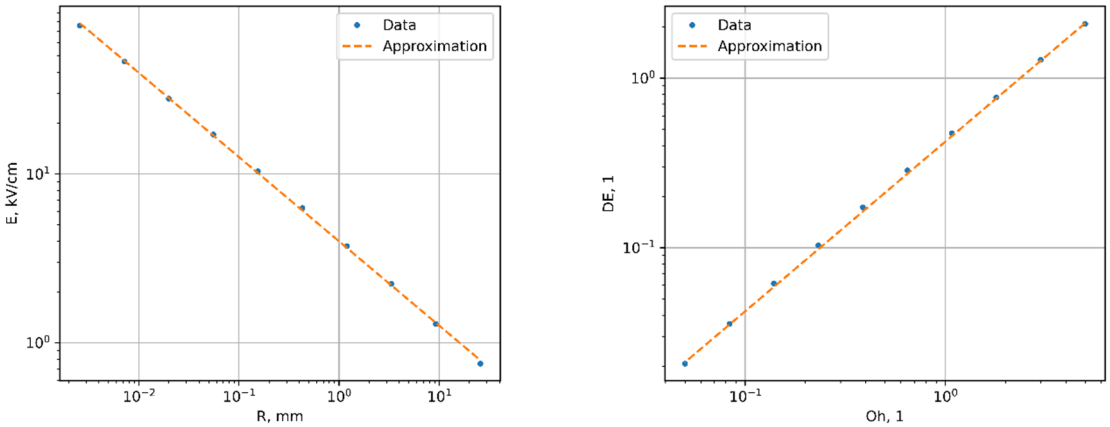

(a) (b)

Figure 3. Results for PDMS50. (a)—Threshold as a function of radius; (b)—Dimensionless threshold as a function of Oh.

In reality, the value of the *We* parameter is not entirely fixed. For each calculated droplet radius, the boundary values of electric field strength at which droplets coalesce and non-coalesce are determined. These values can be used to find the corresponding *We* values. The results are presented in the form of a diagram shown in Figure 4. From this dependency, it can be observed that the critical *We* values for individual radius values, although close to the previously obtained value of 0.178, still differ from it and can vary in the range of approximately 0.17 to 0.20, corresponding to a difference of approximately 10 %.

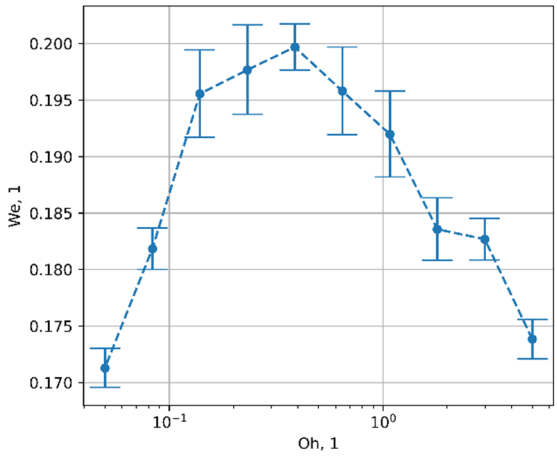

Figure 4. Results for PDMS50. Dependence of the local threshold *We* on *Oh*. The error bars represent the nearest values to the threshold at which coalescence and non-coalescence were numerically obtained.

3.2. Comparison with olive oil

The calculations performed earlier for PDMS50 were repeated for olive oil. It should be noted that the interfacial tension coefficient differs by more than a factor of two between these two liquids. The comparison of results is shown in Figure 5. The nearly complete agreement of data for these two liquids indicates some level of universality in the observed dependencies. This already constitutes a useful outcome and underscores the importance of utilizing dimensionless parameters.

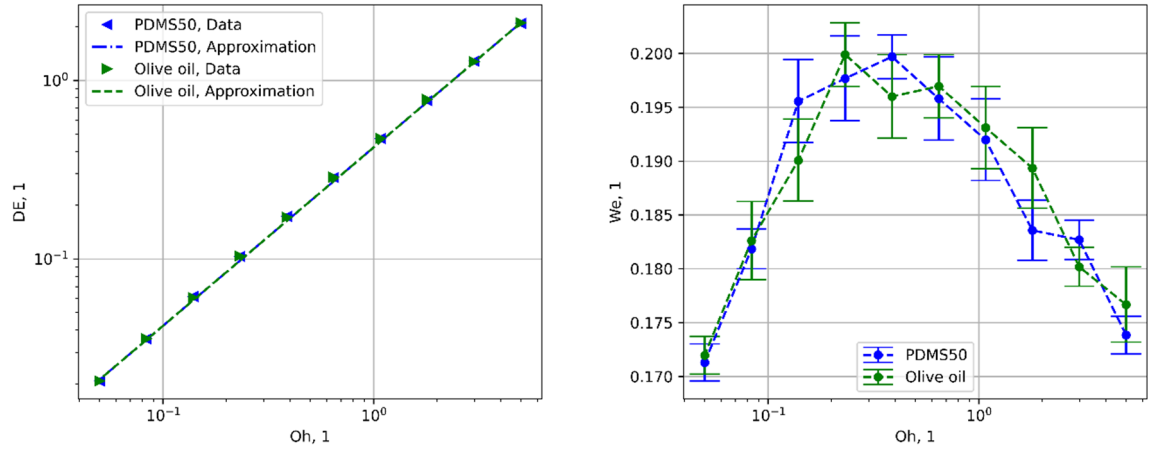

(a) (b)

Figure 5. Results comparison for PDMS50 and olive oil. (a)—the dimensionless threshold as a function of Oh; (b)—the dependence of the local threshold *We* on *Oh*.

3.3. Influence of viscosity

However, the dynamic viscosities of PDMS50 and olive oil are quite close. Dynamic viscosity is an important parameter of the process as it directly influences one of the three forces (electric, surface, viscous). Scaling the viscous forces potentially affects the rate of droplet coalescence by amplifying inertial effects. Moreover, changes in viscosity can lead to alterations in droplet deformation during merging, which may influence the outcome of coalescence. Therefore, to provide a more comprehensive understanding, it is necessary to investigate the influence of viscosity on the observed regularity. Calculations were performed using a liquid similar to PDMS50 but with varied viscosities ranging from 5 to 100 mPa s. The corresponding index was added to the liquid's name in the legend of the plots.

The results of the calculations are shown in Figure 6. It can be observed that all considered viscosity values align well with the previously identified linear dependence of *DE* on *Oh* (Figure 6a). This indicates that, globally, variations in viscosity within the examined range do not significantly impact the outcome of the coalescence process. The dependence of the local threshold *We* on *Oh* (Figure 6b) demonstrates nearly complete agreement for viscosities ranging from 25 to 100 mPa s. For a viscosity of 5 mPa s, the general trend is qualitatively preserved, but a clear quantitative deviation arises.

3.4. Limitation of inter-electrode gap

All previous results were obtained under the assumption that the inter-electrode gap is much larger than the droplet radius, and the inter-electrode gap was scaled along with the droplet radius to maintain a fixed value of the parameter k_d. In reality, small cuvettes and inter-electrode gaps are commonly used in laboratory experiments. This means that the inter-electrode gap may not exceed the droplet radius by several orders of magnitude. To assess how the observed dependencies would change, calculations were performed with a fixed inter-electrode gap of 30 mm.

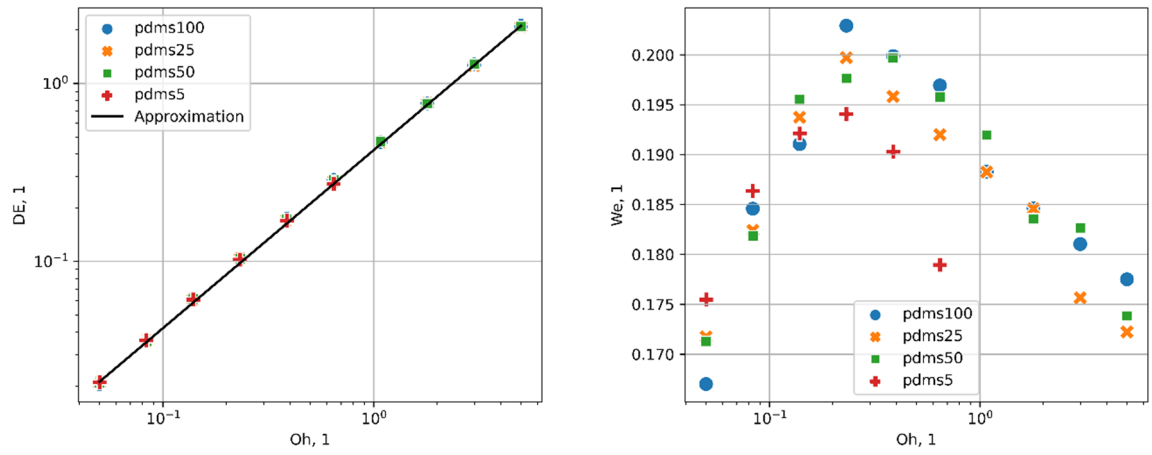

Figure 6. Results comparison for different viscosities of PDMS. (a)—dimensionless threshold as a function of Oh; (b)—the dependence of the local threshold *We* on *Oh*.

The calculated results are shown in Figure 7. The new data points align well with the previously established global dependence of *DE* on *Oh*. For the local dependence of *We* on *Oh*, a qualitative agreement with the previously obtained trend is observed.

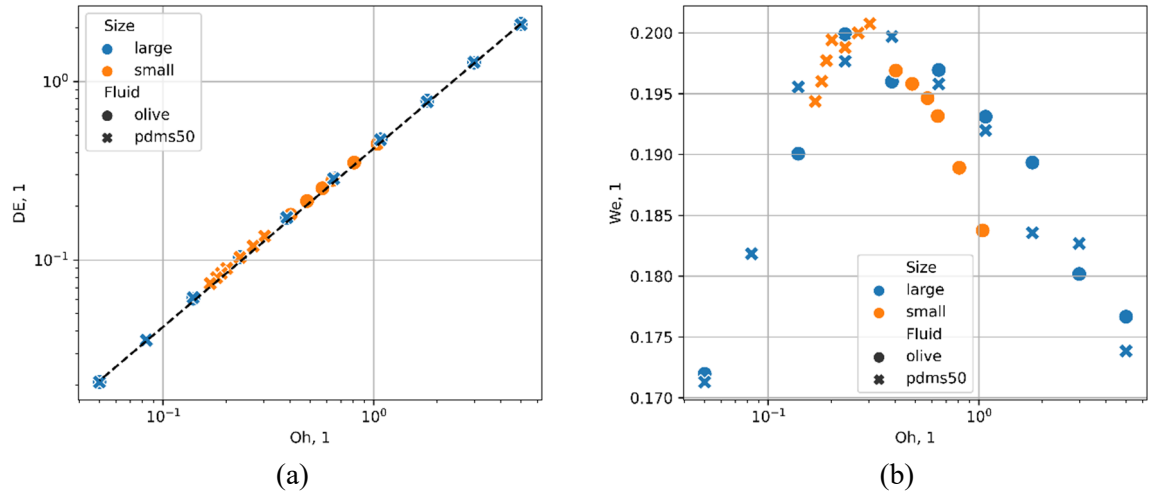

Figure 7. Results comparison for inter-electrode gaps. (a)—dimensionless threshold as a function of *Oh*; (b)—the dependence of the local threshold *We* on *Oh*.

4. Conclusion

Electrocoalescence is a complex multiphysics process influenced by numerous interconnected factors. Depending on these factors, different outcomes can be observed, making predictions challenging. However, it has been discovered that a global regularity can be identified in the dependence of the coalescence threshold on the droplet radius. Exploring such regularities can expedite the acquisition of necessary data regarding the outcomes of the coalescence process and simplify the development of new efficient devices based on this phenomenon.

The identified regularity in the dimensionless analogs of the threshold field strength and droplet radius can aid in experimental planning, particularly when substituting fluids. When seeking the threshold, e.g., if the study focuses on very small droplets, it is possible to select a substitute fluid and investigate an equivalent system with larger droplets.

Acknowledgments
The study was supported by Russian Science Foundation, research project No. 22-79-10078, https://rscf.ru/en/project/22-79-10078/. The research was performed at the Research Park of St. Petersburg State University "Computing Center," "Center for Nanofabrication of Photoactive Materials (Nanophotonics)," and "Center for Diagnostics of Functional Materials for Medicine, Pharmacology, and Nanoelectronics."

References

[1] Mhatre S, Vivacqua V, Ghadiri M, Abdullah A M, Al-Marri M J, Hassanpour A, Hewakandamby B, Azzopardi B and Kermani B 2015 Electrostatic phase separation: A review *Chemical Engineering Research and Design* **96** 177–95

[2] Hadidi H, Kamali R and Manshadi M K D 2020 Numerical simulation of a novel non-uniform electric field design to enhance the electrocoalescence of droplets *European Journal of Mechanics - B/Fluids* **80** 206–15

[3] Tarantsev K V 2013 Modeling of the processes of coagulation and dispersion of water in low-conductive fluids in an electric field *Surf. Engin. Appl.Electrochem.* **49** 414–22

[4] Li B, Wang Z, Vivacqua V, Ghadiri M, Wang J, Zhang W, Wang D, Liu H, Sun Z and Wang Z 2020 Drop-interface electrocoalescence mode transition under a direct current electric field *Chemical Engineering Science* **213** 115360

[5] Chirkov V A, Gazaryan A V, Kobranov K I, Utiugov G O and Dobrovolskii I A 2020 A modification of the phase-field method to simulate electrohydrodynamic processes in two-phase immiscible liquids and its experimental verification *Journal of Electrostatics* **107** 103483

[6] Utiugov G, Chirkov V and Reznikova M 2021 Application of the arbitrary Lagrangian-Eulerian method to simulate electrical coalescence and its experimental verification *International Journal of Plasma Environmental Science and Technology* **15** e02009

[7] Blanchette F and Bigioni T P 2006 Partial coalescence of drops at liquid interfaces *Nature Phys* **2** 254–7

[8] Sunder S and Tomar G 2020 Numerical investigation of a conducting drop's interaction with a conducting liquid pool under an external electric field *European Journal of Mechanics - B/Fluids* **81** 114–23

[9] Pillai R, Berry J D, Harvie D J E and Davidson M R 2017 Electrophoretically mediated partial coalescence of a charged microdrop *Chemical Engineering Science* **169** 273–83

[10] Brik M, Ruscassie R and Saboni A 2016 Droplet deformation and coalescence under uniform electric field *Journal of Chemical Technology and Metallurgy* **51** 649–659

[11] Xu H, Wang T and Che Z 2022 Bridge evolution during the coalescence of immiscible droplets *Journal of Colloid and Interface Science* **628** 869–77

[12] Aryafar H and Kavehpour H P 2006 Drop coalescence through planar surfaces *Physics of Fluids* **18** 072105

[13] Choi S and Saveliev A V 2017 Oscillatory coalescence of droplets in an alternating electric field *Phys. Rev. Fluids* **2** 063603

[14] Mousavichoubeh M, Shariaty-Niassar M and Ghadiri M 2011 The effect of interfacial tension on secondary drop formation in electro-coalescence of water droplets in oil *Chemical Engineering Science* **66** 5330–7

[15] Yang D, Ghadiri M, Sun Y, He L, Luo X and Lü Y 2018 Critical electric field strength for partial coalescence of droplets on oil–water interface under DC electric field *Chemical Engineering Research and Design* **136** 83–93